Cancer Management and Research

Dovepress

open access to scientific and medical research

Open Access Full Text Article

ORIGINAL RESEARCH

HMGB3 silence inhibits breast cancer cell proliferation and tumor growth by interacting with hypoxia-inducible factor 1α

This article was published in the following Dove Press journal:
Cancer Management and Research

Jun Gu
Tao Xu
Qin-Hua Huang
Chu-Miao Zhang
Hai-Yan Chen

Department of Health Check-Up Center, Jinshan Hospital, Fudan University, Shanghai 201508, People's Republic of China

Background: Breast cancer is the most common malignant tumor that affects women with higher incidence. High-mobility group box 3 (HMGB3) plays critical functions in DNA repair, recombination, transcription and replication. This study aimed to investigate the effects of HMGB3 silence on mammosphere formation and tumor growth of breast cancer.

Methods: LV5-HMGB3 and LV3-siHMGB3 vectors were transfected into MCF10A, MDA-MB-231, HCC1937, ZR-75-1 and MCF7 cells. Cell counting kit-8 (CCK-8) assay was used to evaluate cell proliferation. Xenograft tumor mice model was established by injection of MDA-MB-231. qRT-PCR and western blot were used to examine the expression of *Nanog, Sox2* and *OCT-4*. Mammosphere forming assay was employed to evaluate mammosphere formation both in vivo and in vitro. Dual luciferase assay was utilized to verify the interaction between HMGB3 and hypoxia-inducible factor 1α (HIF1α). $CD44^{+}/CD24^{-}$ was assessed with flow cytometry.

Results: HMGB3 expression was higher significantly ($p<0.05$) in cancer cells compared to normal cells. HMGB3 overexpression significantly ($p<0.05$) enhanced and HMGB3 silence reduced cell proliferative mice compared to MCF10A and MDA-MB-231, respectively. HMGB3 overexpression enhanced and HMGB3 silence inhibited mammosphere formation. HMGB3 overexpression upregulated and HMGB3 silence downregulated *Nanog, SOX2* and *OCT-4* genes/proteins in MCF10A and MDA-MB-231 cells, respectively. HMGB3 silence reduced $CD44^{+}/CD24^{-}$ levels in cancer cells. Silence of HMGB3 strengthened reductive effects of PTX on tumor sizes, iPSC biomarkers and mammosphere amounts in xenograft tumor mouse models. HMGB3 silence inhibited mammoshpere formation, cell proliferation and $CD44^{+}CD24^{-}$ by interacting with HIF1α.

Conclusion: HMGB3 silence could inhibit the cell proliferation in vitro and suppress tumor growth in vivo levels. The antitumor effects of HMGB3 silence were mediated by interacting with the HIF1α.

Keywords: HMGB3, breast cancer, HIF1α, mammosphere, proliferation

Introduction

Breast cancer is considered to be the most common malignant tumor that affects women with higher incidence worldwide.[1,2] The metastasis of breast cancer cells is the most important reason for the death of the breast cancer patients.[3] In the recent years, the breast cancer incidence has been increased for 4% in the Chinese females, with more and more urban citizens and more younger population suffering from breast cancer.[4] The triple-negative breast cancer (TNBC) is mainly characterized by the negative expression of HER-2 (ERBB-2), progesterone receptor (PR) and

Correspondence: Tao Xu
Department of Health Check-Up Center, Jinshan Hospital, Fudan University, Longhang Road No.1508, Jinshan District, Shanghai 201508, People's Republic of China
Email liuzheef@sina.com

submit your manuscript | www.dovepress.com
DovePress
http://doi.org/10.2147/CMAR.S204357

estrogen receptor (ER) and accounts for about 10% of total cases of breast cancer.[5,6] The TNBC patients always exhibit poor prognosis because of shortage of efficient therapeutic approaches.[7] Meanwhile, breast cancer metastasis and recurrences occur in appropriately 35% TNBC patients after several years post cancer diagnosis, and the 5-year survival rate of TNBC is only 62% compared to that of the non-TNBC patients (75%).[8,9] Therefore, there is also an urgent need for discovering novel therapeutic approaches and specific drugs against breast cancer, especially for TNBC.

The mammosphere formation has been considered as a marker for the proliferation of the tumor cells.[6,10,11] The mammosphere cell culture, producing spherical colonies, has been extensively applied to investigate the properties of the progenitor cells by evaluating biomarkers, such as CD44, CD49 and CD24.[12,13] Ma et al[14] found that CD44(+)/CD24(–) cell population is enriched in TNBC and plays a critical role in aggressive behaviors of breast cancer. Rappa and Lorico[15] discovered that the mammospheres derived from the breast cancer cell MA-11 exhibited a significantly higher oncogenic capability compared to that of normal cells. Grimshaw et al[16] also reported that 20 of 27 breast cancer patients formed the mammospheres and demonstrated obviously expanded and differential capability. Meanwhile, the majority of mammospheres are phenotypically CD44(+)/CD24(–) cell population.[17]

Therefore, in this study, we evaluated the proliferation of breast cancer by assessing the formation of the mammospheres. Moreover, a previous study reported that breast cancer patients usually exhibited higher expressions of hypoxia-inducible factor 1α (HIF1α)[18] and higher levels of HIF1α indicated a poor prognosis for breast cancer patients.[19] Therefore, we also determined the HIF1α expression in this study.

High-mobility group box 3 (HMGB3), also called HMG2a, is a member of HMGB family, which plays critical functions in DNA repair, recombination, transcription and replication.[20] Previous studies[21-23] also reported that HMGB3 participated in the progression of a few cancers, including gastric, bladder, lung and esophageal cancers. Meanwhile, the HMGB3 is highly expressed in tumor tissues and is involved in the recurrence, metastasis and drug resistance of many cancers.[24–26] The HMGB3 also enhances the proliferation of cancers and cancer stem cells.[27,28] Also, a previous study[26] reported that the miRNA-205 could inhibit the breast cancer cell proliferation by regulating HMGB3, but have not studied the effects of HMGB3 directly on breast cancer. Moreover, the effects of HMGB3 on the proliferation, chemoresistance, invasion and migration have not been fully clarified and the mechanism of the above effects is still elusive in breast cancer. Therefore, in this study, we investigated the effects of HMGB3 silence on mammosphere formation and tumor reoccurrence in both breast cancer cells and xenograft tumor models.

Materials and methods

Cells and culture

The normal breast cell line, MCF10A, and the human breast cancer cell lines, MDA-MB-231, HCC1937, ZR-75-1 and MCF7, were purchased from Cell Bank of the Chinese Academy of Science (Shanghai, China). MCF10A cells were cultured in mammary epithelial cell growth (MEGM) (Gibco BRL. Co. Ltd., Grand Island, NY, USA), MDA-MB-231 cells were cultured in L-15 medium (Gibco BRL. Co. Ltd.), HCC1937 and ZR-75-1 cells were cultured in RPMI 1640 (Gibco BRL. Co. Ltd.), MCF7 cells were cultured in minimum eagle medium (MEM) (Gibco BRL. Co. Ltd.), supplemented with FBS (Gibco BRL. Co. Ltd.) and 1% penicillin–streptomycin (Beyotime Biotech. Shanghai, China) in a humidified incubator at 37 ℃ with 5% CO_2.

This study was approved by the Ethics Committee of Jinshan Hospital, Fudan University, Shanghai, China.

Plasmid construction, lentivirus packaging and transfection into cells

pG-LV5 and pG-LV3 lentiviral vector (LV5 and LV3 vector, purchased from GenePhama Co. Ltd, Shanghai, China) were utilized to establish the LV5-HMBG3 and LV3-siHMGB3, respectively. Oligonucleotides for HMGB3 mimic gene and HMGB3 siRNA gene were synthesized by GenePhama Co. Ltd. The sense and antisense sequences for HMGB3 siRNA were listed as follows: sense 5‘-GATCC-(GN_{18})-(TTCA AGAGA)-(N_{18}C)-TTTTTG-3‘, antisense 3‘-G(CN_{18})-(AAG TTCTCT)-(N_{18}G)-AAAAAACTTAA-5‘. The targeting sequence for HMGB3 siRNA is as follows: TGAGAA GGATGTTGCTGACTATA. The sense and antisense sequences for HMGB3 mimic were listed as follows: sense 5‘-AGGGTTCCAAGCTTAAGCGGCCGCGCCACCATGG CTAAAGGT GACCCCAAGAAAC-3‘, antisense 5‘- GAT CCATCCCTAGGTAGATGCATTTA TTCATCCTCCTCCT CCTCCTCCTCCTCT-3‘. The DNA double-chains were artificially synthesized by GenePhama Co. Ltd. Eventually, the synthesized double-chain sequences for both HMGB3 mimic

and HMGB3 siRNA were subcloned into pG-LV5 and pG-LV3 plasmid to establish the LV5-HMGB3 and LV3-siHMGB3 plasmid, respectively.

LV5-HMGB3/LV3-siHMGB3 plasmid and the packing plasmids (PG-p1-VSVG, PG-P2-REV, PG-P3-RRE) were transfected with the RNAi-mate (GenePhama Co., Ltd), based on manufacturer' instruction. The processes of viral packaging were performed as previously described.[29]

The breast cancer cell lines were infected with LV5-HMGB3 and LV3-siHMGB3 plasmid, at the final multiplicity of infection (MOI) of 15,[2] supplemented with 5 μg/mL polybrene (GenePhama Co. Ltd) treatment. Finally, viral vector infective efficiency was evaluated with microscopic analysis for green fluorescent protein (GFP) fluorescence.

Cell counting kit-8 (CCK-8) assay

Cell proliferative rates of MCF10A, MDA-MB-231, HCC1937, ZR-75-1 and MCF7 were evaluated with the CCK-8 (Cat. No. 96992, Sigma-Aldrich, St. Louis, MO, USA) according to the instruction of the manufacturer. The above breast cancer cells were seeded onto 96-well plates (Corning-Costar, Corning, NY, USA) containing media (with a final density of 1×10^5 cells/mL) and transfected with LV5-HMGB3 or LV3-siHMGB3 lentivirus. Then, the breast cancer cells were cultured for 24 hrs, 48 hrs and 72 hrs and incubated with CCK-8 regent at a final concentration of 10 μL/mL for 4 hrs at 37°C. At last, cell proliferative rates of breast cancer cells were evaluated using a microplate reader (Thermo Fisher Scientific, Hudson, NH, USA) at 450 nm wavelength.

qRT-PCR

RNAs of the breast cancer cells were extracted using Trizol reagents, which were purchased from Beyotime Biotech (Shanghai, China). The purity and concentration of the isolated RNA were evaluated by examining OD260/OD280 values with micro-spectrophotometer method. The integrity of isolated RNA was determined using capillary electrophoresis method. The commercial reverse transcription reagents purchasing from Western Biotech (Chongqing, China) were applied to synthesize the complementary DNAs (cDNAs) based on the instruction of the manufacturer. The qRT-PCR assay was performed using the commercial Sybgreen I kit (Western Biotech) based on the instruction of manufacturer and conducted using a real-time PCR system (Mode: FTC-3000P, Funglyn Biotech, Toronto, Canada). Amplification conditions for the qRT-PCR were performed as follows: 4 mins at 94°C, 20 s at 94°C, 30 s at 60°C, 30 s at 72°C, for 35 cycles. The qRT-PCR primers for *Nanog, Sox2, OCT-4* and *β-actin* are listed in Table 1. The present qRT-PCR is the one-step RT-PCR. Finally, the amplified products of the above genes were loaded onto the 1.5% agarose gels (Beyotime Biotech) and the images were analyzed using the GDS8000 UVP image scanning system (Sacramento, CA, USA). The melting curve was drawn and the efficiency of qRT-PCR was assessed (with higher efficiency). The relative gene levels were normalized to β-actin gene by employing the previously introduced comparative threshold cycle ($2^{-\triangle\triangle CT}$) method.[30]

Mammosphere forming assay

The mammosphere forming assay was conducted according to the previously established protocol.[31] Briefly, the breast cancer cells were cultured to a density of 50–60% confluence and detached using the StemPro Accutase (Invitrogen/Life Technologies, Carlsbad, CA, USA). The breast cancer cells were then cultured on the 6-well plates (Corning-Costar, Corning, NY, USA) at a density of 10,000 cell/mL and maintained in the medium supplemented with heparin and hydrocortisone. The primary mammospheres were collected and enzymatically dissolved using the StemPro Accutase. Then, the breast cancer cells were re-plated for the subsequent passages at a final density of 5,000 cells/mL. The images of the mammospheres were taken and the mammosphere formation was calculated by comparing with the accounts of MCF10A or MDA-MB-231 cells according to the previously published study.[13]

Dual luciferase assay

In order to evaluate the interaction between HMGB3 expression and HIF1α expression, the dual luciferase assay was performed in the 293T cells (Shanghai Cell Bank of China Academia Sinica, Shanghai, China). About 48 hrs after the

Table 1 Sequences for the RT-PCR assay

Genes	Sequences	Length (bp)
HMGB3	ACAGTGAAAAGCAGCCTTACATC CGGGCAACTTTAGCAGGAC	124
Nanog	ATGGATCTGCTTATTCAGGACAG GTTTCTTGACCGGGACCTTG	115
Sox2	AGTGGAAACTTTTGTCGGAGAC GCAGCGTGTACTTATCCTTCTTC	150
OCT-4	AAGGGCAAGCGATCAAGC AAGGGACCGAGGAGTACAGTG	166
β-actin	TGACGTGGACATCCGCAAAG CTGGAAGGTGGACAGCGAGG	205

Abbreviation: HMGB3, high-mobility group box 3.

pGL3-HIF1α-promoter and pcDNA3.1-HMGB3, luciferase activity was assessed with a Dua-Luciferase Reporter Assay System (Cat. No. E1910, Promega, Madison, MI, USA) according to the manufacturer's instruction. Then, the fluorescence intensity of the dual luciferase assay was determined with a microplate reader (Mode: MCC/340, Thermo Fisher Scientific). Finally, the luciferase activities were calculated by comparing with the values of the Renilla luciferase plasmid.

Western blot assay

The breast cancer cells were digested and lyzed with the RIPA solution (Biyotime Biotech). The digested products were centrifuged at 4°C for 5 mins at 10,000 r/min to obtain the proteins. The proteins were separated using the 15% SDS-PAGE (Beyotime Biotech) and electrotransferred onto the polyvinylidene floride (PVDF) membrane (Amersham Biosciences, Piscataway, NJ, USA) by utilizing a Trans-Blot Semi-Dry Electrophoretic Transfer (Mode: 170–3940, Bio-Rad Laboratories, Hercules, CA, USA). The rabbit anti-human Nanog monoclonal antibody (1: 3,000; Cat. No. ab109250, Abcam Biotech, Cambridge, MA, USA), rabbit antihuman Sox2 polyclonal antibody (1:2,000, Cat No. ab137385, Abcam Biotech), rabbit antihuman OCT-4 polyclonal antibody (1:2,000, Cat No. ab137427, Abcam Biotech), rabbit antihuman HIF-1α monoclonal antibody (1:3,000, Cat No. ab179483, Abcam Biotech) and rabbit antihuman β-actin polyclonal antibody (1: 2,000; Cat. No. ab228001, Abcam Biotech) were utilized to treat the protein transferred PVDF membranes at 4 ℃ overnight. The PVDF membranes were washed using the PBS (Hyclone, Logan, UT, USA) for 5 mins and 3 times per minute and incubated using the horse radish peroxidase (HRP)-labeled goat anti-rabbit IgG (1: 2,000, Cat. No. AQ132P, Sigma-Aldrich) at room temperature for 2 hrs. Then, PVDF membranes were treated using BeyoECL Star kit (Cat. No. P0018AFT, Beyotime Biotech) in dark for 2 mins at room temperature. Eventually, the western blot bands were captured using Gel Analysis System (Mode: Tannon-4200, Tanon Sci. Tech. Co. Ltd., Shanghai, China) and analyzed using a 4.0 Labworks™ Analysis Software (Labworks, Upland, CA, USA).

Flow cytometry assay for evaluating $CD44^+/CD24^-$

The $CD44^+/CD24^-$ cells were analyzed and identified according to the previous study.[32] In brief, the breast cancer cells were washed and then trypsinized into the single-cell suspensions. The PE-conjugated antihuman CD44 monoclonal antibody (Cat. No. #12-0441-82, eBioscience, Santiago, CA, USA) and APC conjugated anti-human CD24 monoclonal antibody (Cat No. #17-0247-42, eBioscience, Santiago, CA, USA) were added into the breast cancer cell suspension in dark and at 4°C for 30 mins, according to the instruction of manufacturer. In order to eliminate the unbound antibodies, the labeled cells were washed using PBS. Finally, the cells were analyzed on a FACSCanto II Flow Cytometry (BD Biosciences, San Jose, CA, USA) within 1 hr poststaining.

Xenograft tumor assay

The BALB/C nude mice (6–8 weeks, weighing from 20 g to 25 g) were purchased from Tengxin Biotech. Co. Ltd. (Chongqing, China). The MDA-MB-231 cells were adjusted to the density of 1×10^7 cells/mL in L-15 medium (Gibco BRL. Co. Ltd.) to generate the MDA-MB-231 cell suspension. Then, 1 mL of cell suspension was injected subcutaneously into the flanks of mice. The tumor sizes in single MDA-MB-231 group, paclitaxel (PTX) group, PTX +siRNA-NC group and PTX+siHMGB3 group were measured and calculated with a formula of $(\text{length}\times\text{width}^2)/2$. The isolated tumor tissues were used to evaluate Nanog, Sox2 and OCT-4 expression using immunofluorescence assay. Meanwhile, the tumor tissues were also employed to determine the mammosphere formation using H&E staining according to the previously published study.[33]

The mice experiments in the present study were conducted according to Guide for the Care and Use of Laboratory Animals of National institute of Health. The animal experiments or tests were also approved by the Ethics Committee of Jinshan Hospital, Fudan University, Shanghai, China.

HIF1α mimic and HIF1α siRNA plasmid synthesis and transfection

The HIF1α-siRNA sequence was designed using the BLOCK-iT RNAi Designer. The sequence was listed as follows: GAGGAAACUUCUGGAUGCU GGUGAUTT. The sequence was annealed using their complementary sequence, subcloned into the pcDNA3.1 (+) vector (Cat. No. V79020, Invitrogen/Life Technologies, Carlsbad, CA, USA) and then transfected into the MCF10A cells and MDA-MB-231 cells. The full-length HIF1α codon sequence was then subcloned into the pcDNA3.1 vector and then transfected into the MCF10A cells and MDA-MB-231 cells.

Immunofluroescent assay

The cancer tissues were fixed with 4% paraformaldehyde (Sigma-Aldrich) in PBS, cryoprotected in 30% sucrose in PBS for 48 hrs and then frozen. Then, the cancer tissues were cut into section at thickness of 10 μm and blocked using 1% BSA (Beyotime Biotech) containing 0.05% Triton X-100 for 60 mins. The sections were treated with rabbit antihuman Nanog monoclonal antibody (1: 3,000; Cat. No. ab109250), rabbit antihuman Sox2 polyclonal antibody (1:2,000, Cat No. ab137385), rabbit antihuman OCT-4 polyclonal antibody (1:2,000, Cat No. ab137427) at 4℃ overnight. The sections were then incubated with goat antirabbit Alexa Fluor fluorescein (FITC)-labeled IgG (1:1,000, Cat. No.ab6717) at room temperature for 2 hrs. All of the above first antibodies and second antibody were purchased from Abcam Biotech . The nuclei were stained with DAPI (Beyotime Biotech). The stained images were captured using fluorescent microscope (Mode: BX51; Olympus, Tokyo, Japan).

Statistical analysis

Data in this study were represented as the definition of mean ± SD and analyzed with SPSS software 20.0 (SPSS Inc., Chicago, IL, USA). Differences between two groups were analyzed with Student's *t* test, and the differences among multiple groups were analyzed using Tukey's post-hoc test validated ANOVA analysis. All of the experiments or tests were conducted at least 6 repeats. The *p*-values <0.05 were assigned as significant difference.

Results

HMGB3 highly expressed in breast cancer cell lines

In order to identify and compare the levels of HMGB3 in the breast cancer cells and normal cells, the HMGB3 expressions were examined using qRT-PCR assay. The results showed that HMBG3 expression in basal-like cell lines (MDA-MB-231, HCC1937) was significantly higher compared to that in MCF10A cells (Figure 1A, $p<0.05$). The HMBG3 expression in luminal cell lines (ZR-75-1, MCF7) was also significantly higher compared to that in MCF10A cells (Figure 1B, $p<0.05$). Moreover, the HMGB3 expression in basal-like cell lines (MDA-MB -231, HCC1937) was also significantly higher compared to that in luminal cell lines (ZR-75–1, MCF7) (Figure 1C, $p<0.05$).

HMGB3 overexpression enhanced cell proliferation of MCF10A cells and HMGB3 silence reduced cell proliferation of MDA-MB-231 cells

To clarify the effects of overexpression of HMGB3 on normal breast cells and effects of HMGB3 silencing of HMGB3 on breast cancer MDA-MB-231 cells, the qRT-PCR assay was conducted. The results indicated that HMGB3 overexpression significantly enhanced (Figure 2A) and HMGB3 silence significantly reduced (Figure 2B) HMGB3 levels compared to MCF10A+LV5 cells and MDA-MB-231-LV3 cells, respectively ($p<0.05$).

Our results also demonstrated that the HMGB3 overexpression significantly enhanced cell proliferation of MCF10A cells compared to that in MCF10A+LV5 cells without LV5-HMGB3 transfection at 72 hrs post-treatment (Figure 2C, $p<0.0.5$). Meanwhile, HMGB3 silence significantly reduced cell proliferation of MDA-MB-231 cells compared to that in MDA-MB-231-LV3 cells without LV3-siHMGB3 transfection at 72 hrs post-treatment (Figure 2D, $p<0.05$).

HMGB3 overexpression enhanced and HMGB3 silence inhibited mammosphere formation

Because the mammosphere forming reflects the tumor cell proliferation,[25] the mammosphere formation assay was performed. The results indicated that HMGB3 overexpression significantly increased the amounts of mammospheres in MCF10A cells compared to that in MCF10A+LV5 cells without LV-5HMGB3 treatment (Figure 3A, $p<0.05$). Meanwhile, HMGB3 silence significantly decreased the amounts of mammospheres in MDA-MB-231 cells compared to that in MDA-MB-231+LV3 cells without LV-3-siHMGB3 treatment (Figure 3B, $p<0.05$).

HMGB3 overexpression upregulated Nanog, SOX2 and OCT-4 in MCF10A cells

The biomarkers for the induced pluripotent stem cells (iPSCs),[34] such as Nanog, SOX2 and OCT-4, were examined using qRT-PCR assay and western blot assay. The qRT-PCR assay results showed that expression of *Nanog, SOX2* and *OCT-4* genes was significantly increased in MCF10+LV5-HMGB3 group compared to that in MCF10A-LV5 group (Figure 4A, $p<0.05$). Meanwhile, the western blot assay also indicated that expression of

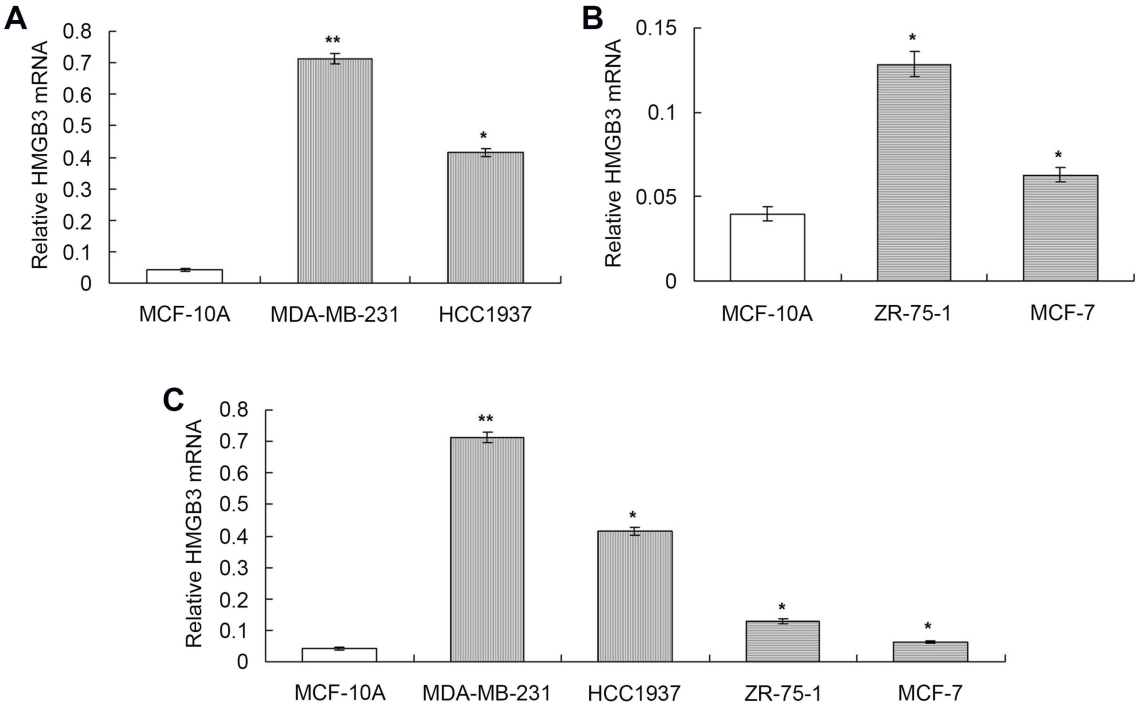

Figure 1 Determination of mRNA expression of HMGB3 in different breast cancer cells using qRT-PCR assay. (**A**). Statistical analysis for HMGB3 mRNA in MCF10A, MDA-MB-231 and HCC1937 cells. (**B**). Statistical analysis for HMGB3 mRNA in MCF10A, ZR-75-1 and MCF7 cells. (**C**). Statistical analysis for HMGB3 in all of the normal cells and breast cancer cells. *p<0.05, **p<0.01 *vs* MCF10A cells.
Abbreviation: HMGB3, High-mobility group box 3.

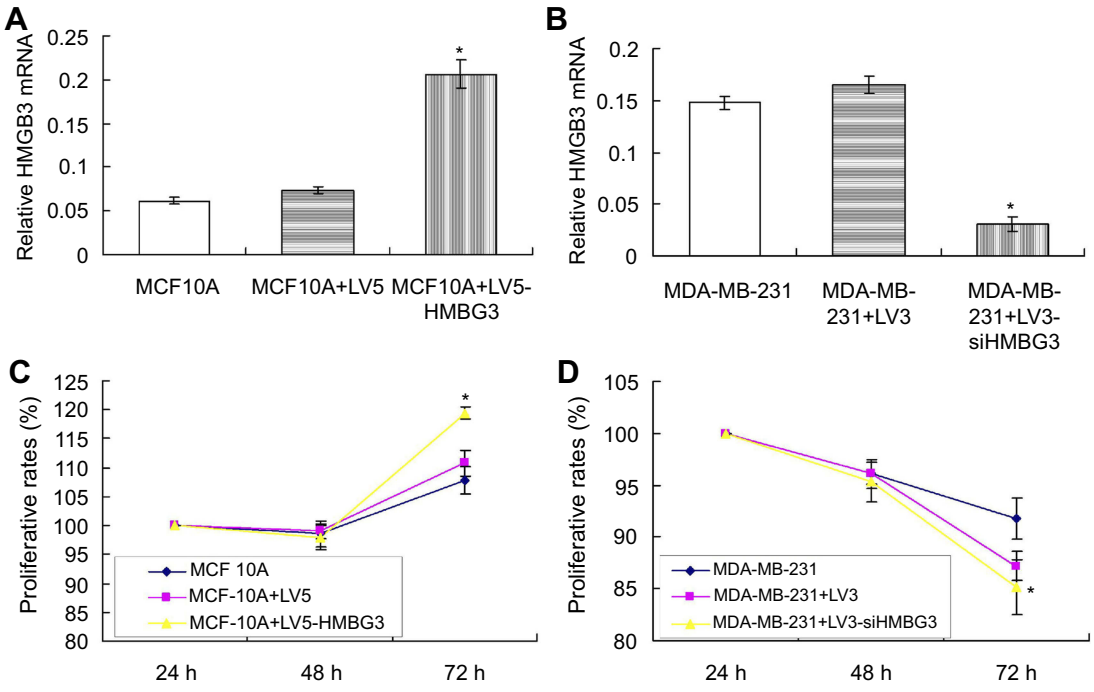

Figure 2 Effects of HMGB3 overexpression on MCF10A proliferation and HMGB3 silence on MDA-MB-231 proliferation. (**A**). Statistical analysis for HMGB3 mRNA in HMGB3-treated MCF10A cells. (**B**). Statistical analysis for HMGB3 mRNA in siHMGB3-treated MDA-MB-231 cells. (**C**). Effects of HMGB3 overexpression on MCF10A proliferation at 24 hrs, 48 hrs and 72 hrs. (**D**) Effects of HMGB3 silence on MDA-MB-231 proliferation at 24 hrs, 48 hrs and 72 hrs. *p<0.05 vs MCF10A-LV5 cells or MDA-MB-231-LV3 cells.
Abbreviation: HMGB3, High-mobility group box 3.

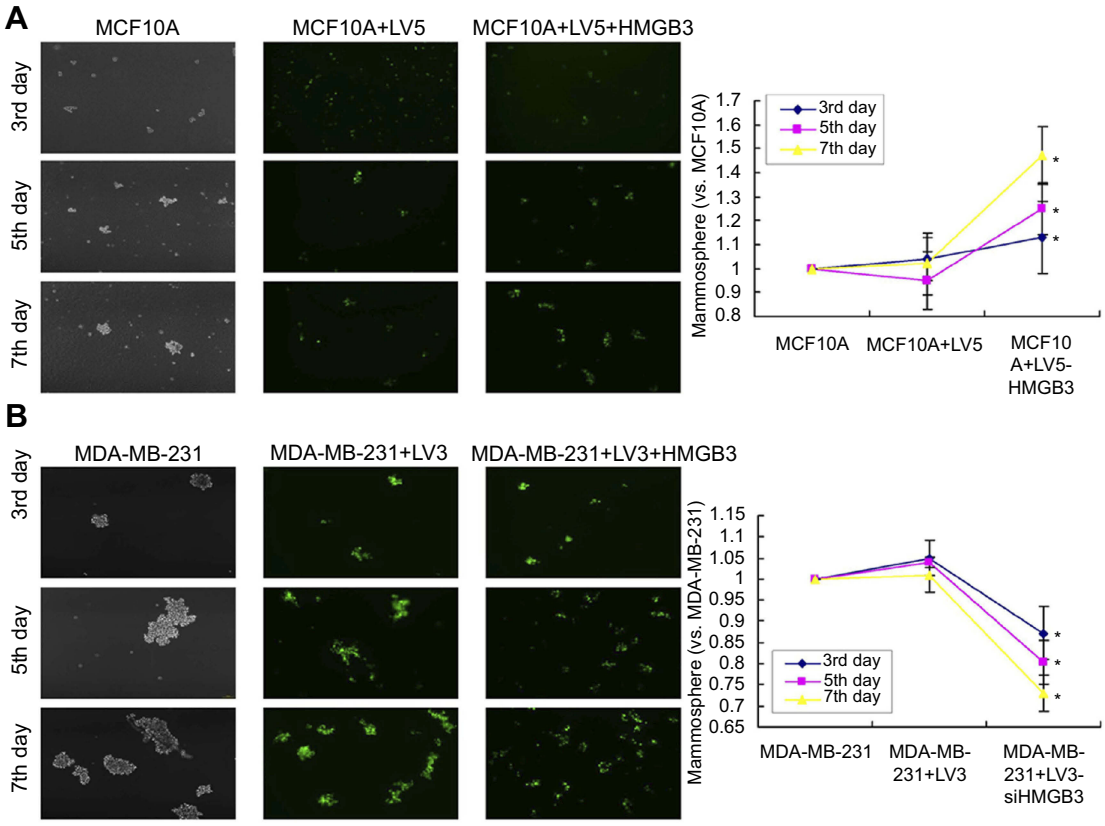

Figure 3 Mammosphere formation in the HMGB3-treated MCF10A cells and siHMGB3-treated MDA-MB-231 cells. (**A**). Images and statistical analysis for mammosphere formation in HMGB3-treated MCF10A cells. Scale bar: 100×. (**B**). Images and statistical analysis for mammosphere formation in siHMGB3-treated MDA-MB-231 cells. *p<0.05 *vs* MCF10A-LV5 cells or MDA-MB-231-LV3 cells.
Abbreviation: HMGB3, High-mobility group box 3.

Nanog, SOX2 and OCT-4 was significantly enhanced in MCF10+LV5-HMGB3 group compared to that in MCF10A-LV5 group (Figure 4B, p<0.05).

HMGB3 silence downregulated Nanog, SOX2 and OCT-4 in MDA-MB-231 cells

The qRT-PCR assay results showed that expression o*f Nanog, SOX2* and *OCT-4* was significantly decreased in MDA-MB -231-LV3-siHMGB3 group compared to that in MDA-MB -231-LV3 group (Figure 4A, p<0.05). Meanwhile, the western blot assay also indicated that expression of Nanog, SOX2 and OCT-4 was significantly reduced in MDA-MB-231-LV3-siHMGB3 group compared to that in MDA-MB-231-LV3 group (Figure 4B, p<0.05).

HMGB3 played critical role in regulating $CD44^+/CD24^-$ cells

In order to evaluate the effects of HMGB3 on the tumor cells initiation, the levels of $CD44^+/CD24^-$ cells were analyzed using flow cytometry assay. The results indicated that HMGB3 overexpression significantly up-regulated the $CD44^+/CD24^-$ cells levels in MCF10A cells compared to the MCF10A-LV5 cells without LV5-HMGB3 treatment (Figure 5A, p<0.05). Moreover, the HMGB3 silence significantly down-regulated the $CD44^+/CD24^-$ cells levels in MDA-MB-231-LV3 cells compared to the cells untreated with LV3-siHMGB3 (Figure 5B, p<0.05).

Silence of HMGB3 strengthened the reductive effects of PTX on tumor sizes in xenograft tumor mouse models

The natural antitumor drug, PTX, and the siHMGB3 were administrated to the MDA-MB-231-induced xenograft tumor mouse models to observe the effects on tumor sizes (Figure 6A). The results showed that PTX significantly decreased the tumor sizes of tumor models compared to that in xenograft tumor model without siHMGB3 treatment (Figure 6B, p<0.05). What's most important, siHMGB3 combining PTX illustrated even more significant effects compared to the PTX

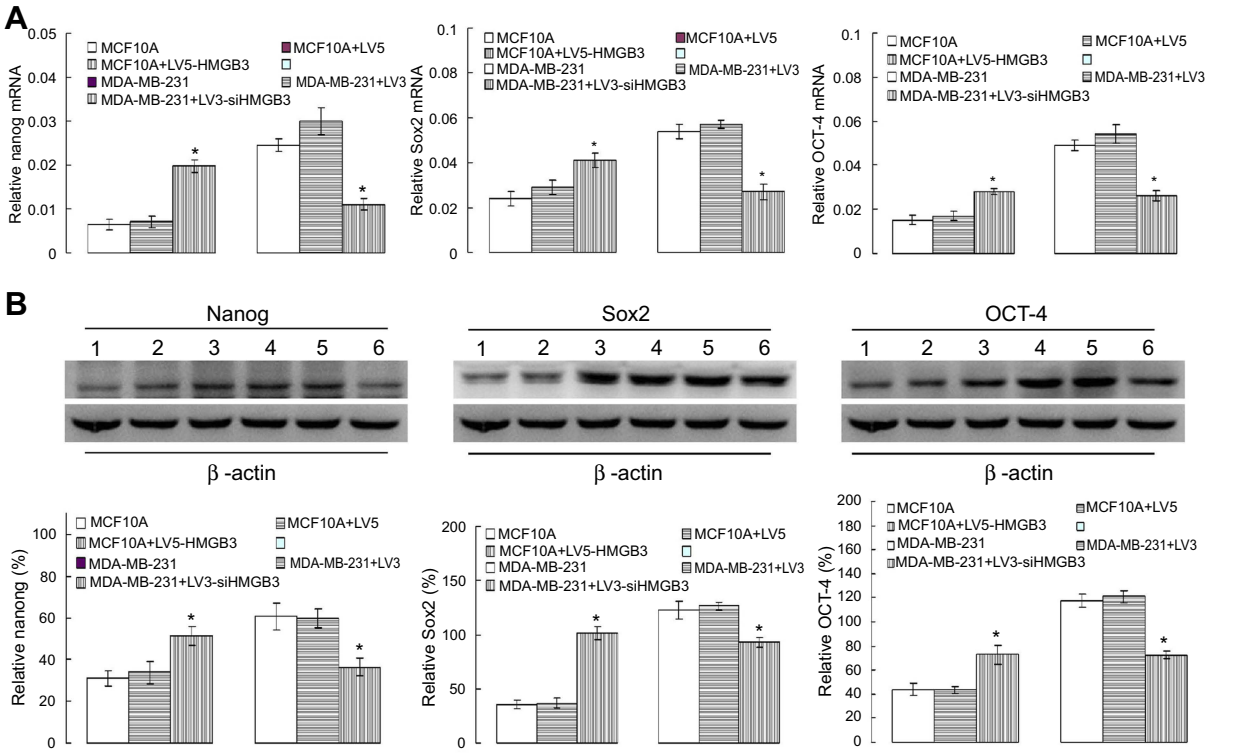

Figure 4 Evaluation of Nanog, Sox2 and OCT-4 mRNA and protein expression using qRT-PCR and western blot assay. (**A**). Statistical analysis for the *Nanog*, *Sox2* and *OCT-4* mRNA expression in HMGB3-treated MCF10A and siHMGB3-treated MDA-MB-231 cells using qRT-PCR assay. (**B**). Statistical analysis for the Nanog, Sox2 and OCT-4 expression in HMGB3-treated MCF10A and siHMGB3-treated MDA-MB-231 cells using western blot assay. *p<0.05 *vs* MCF10A-LV5 cells or MDA-MB-231-LV3 cells. The number 1–6 represent the MCF10A, MCF10A+LV5, MCF10A+LV5+HMGB3, MDA-MB-231, MDA-MB-231+LV3 and MDA-MB-231+LV3-siHMGB3, respectively.
Abbreviation: HMGB3, High-mobility group box 3.

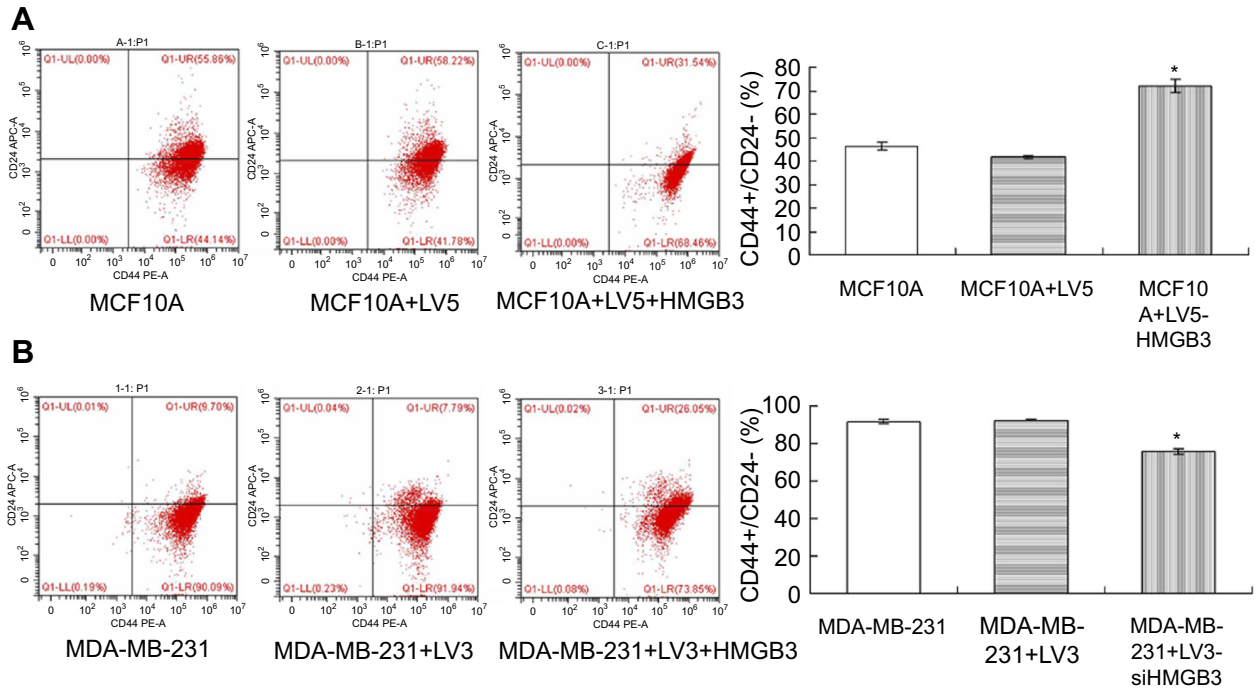

Figure 5 $CD44^+/CD24^-$ levels detection in MCF10A and MDA-MB-231 cells with flow cytometry assay. (**A**). $CD44^+/CD24^-$ evaluation in HMGB3-treated MCF10A cells. (**B**). $CD44^+/CD24^-$ evaluation in siHMGB3-treated MDA-MB-231 cells. *p<0.05 *vs* MCF10A-LV5 cells or MDA-MB-231-LV3 cells.
Abbreviation: HMGB3, High-mobility group box 3.

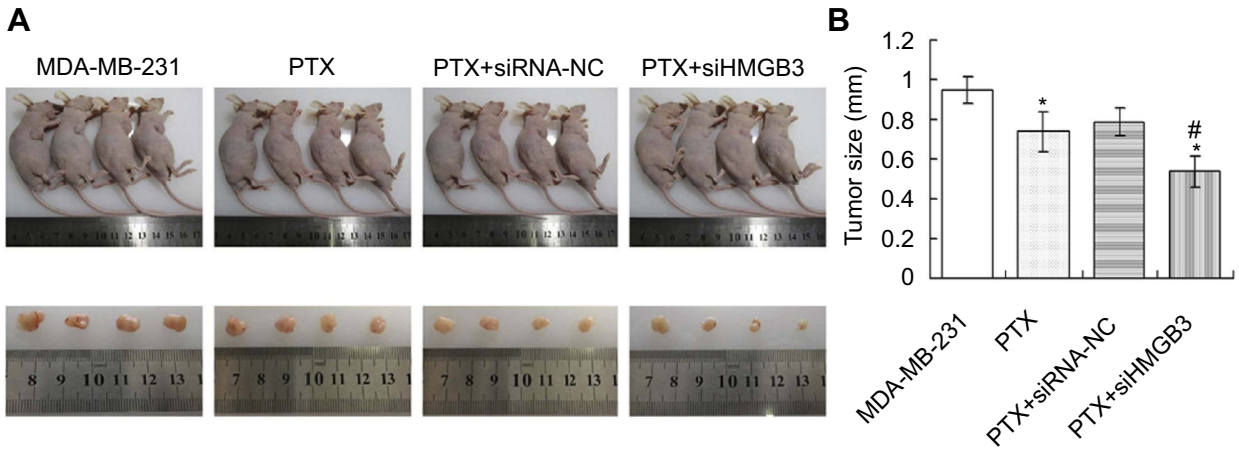

Figure 6 Tumor size calculation of the PTX and/or siHMGB3-treated xenograft tumor mice models. (**A**). Xenograft tumor mice models with tumors and the isolated tumors. (**B**). Statistical analysis for the tumor sizes. $^{*}p<0.05$ *vs* MDA-MB-231 cells. $^{\#}p<0.05$ *vs* PTX group.
Abbreviation: HMGB3, High-mobility group box 3.

treatment on the tumor size inhibition (Figure 6B, $p<0.05$).

Silence of HMGB3 strengthened downregulatory effects of PTX on iPSCs biomarkers and mammosphere amounts

Our data showed that PTX significantly decreased the CD44, Nanog, Sox2 and OCT-4 levels and mammosphere amounts in tumor tissues of mouse models ($p<0.05$). However, the CD44, Nanog, Sox2 and OCT-4 expression was significantly lower in PTX+siHMGB3 group (or PTX group) compared to that in PTX+siRNA-NC group (Figure 7A, $p<0.05$). Meanwhile, the mammosphere amounts were significantly decreased in PTX+siHMGB3 group (or PTX group) compared to that in PTX+siRNA-NC group (Figure 7B, $p<0.05$).

HMGB3 silence inhibited HIF1α expression in MDA-MB-231 cells

It is well known that HIF1α plays critical roles in the tumor cell growth; therefore, we evaluated the expression of HIF1α in the MDA-MB-231 cells by both qRT-PCR assay and western blot assay. The results showed that HMGB3 overexpression significantly increased mRNA (Figure 8A) and protein (Figure 8B) levels of HIF1α compared to that in MCF10A-LV5 group and MCF10A groups ($p<0.05$). Moreover, the silence of HMGB3 significantly reduced the mRNA (Figure 8A) and protein (Figure 8B) expressions of HIF1α compared to that in MDA-MB-231-LV3 group and MDA-MB-231 groups ($p<0.05$).

HIF1A silence inhibited mammosphere formation and decreased $CD44^{+}/CD24^{-}$ levels in MCF10A cells

The mammosphere formation assay (Figure 9A) was conducted in MCF10A cells undergoing siHIF1α and MDA-MB-231 cells undergoing HIF1α treatment. Our results exhibited that siHIF1α transfection significantly decreased the mammosphere amounts in MCF10A-LV-5-HMGB3 cells compared to that in the cells without HMGB3 treatment (Figure 9B, $p<0.05$). Also, HIF1α silence significantly decreased the $CD44^{+}/CD24^{-}$ levels in MCF10A+LV5-HMGB3 cells compared to that without siHIF1α treatment (Figure 10A, $p<0.05$).

HIF1α overexpression triggered mammosphere formation and enhanced $CD44^{+}/CD24^{-}$ levels in MDA-MB-231 cells

The results illustrated that HIF1α overexpression significantly triggered the mammosphere formation in MDA-MB-231-LV-3-siHMGB3 cells compared to that in cells without HIF1α treatment (Figure 9C, $p<0.05$). Also, HIF1α overexpression significantly enhanced the $CD44^{+}/CD24^{-}$ levels in MDA-MB-231-LV-3-siHMGB3 cells compared to that without HIF1α treatment (Figure 10B, $p<0.05$).

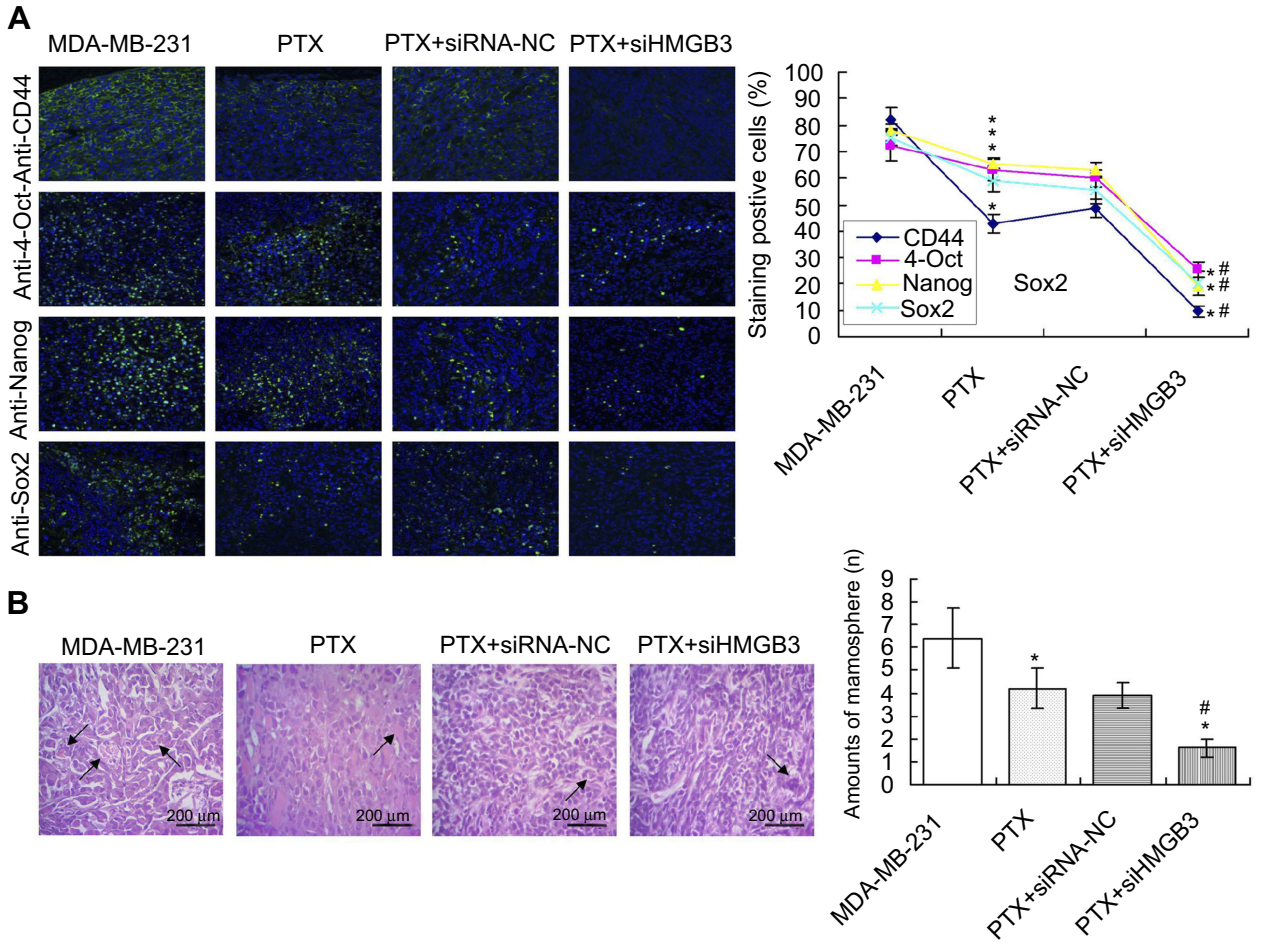

Figure 7 Examination for the Nanog, Sox2 and OCT-4 expression and mammosphere formation evaluation in tumor tissues of xenograft tumor mice models. (**A**). Nanog, Sox2 and OCT-4 expression was examined with immunofluorescence assay. Scale bar: 400×. (**B**). Mammosphere formation evaluation in tumor tissues. *p<0.05 *vs* MDA-MB-231 cells. #p<0.05 vs PTX group.
Abbreviation: HMGB3, High-mobility group box 3.

HMGB3 interacted with HIF1α in MDA-MB-231 cells

The dual luciferase assay results indicated that when co-transfected with both pGL3-HIF1α-promoter and pcDNA3.1-HMGB3, there were no significant differences for luciferase activity between MCF10A cells and MDA-MB-231 cells (Figure 11, p<0.05). However, when transfected with only pGL3-HIF1α-promoter, the luciferase activity was significantly higher in MDA-MB-231 cells compared to that in MCF10A cells (Figure 11, p<0.05). The luciferase activities in pGL3-HIF1α-promoter and pcDNA3.1-HMGB3 co-transfection group (both MCF10A and MDA-MB-231 cells) were higher significantly compared to that in the normal control cells (without transfection, Figure 11, p<0.05). The luciferase activities in pGL3-HIF1α-promoter transfection group (both MCF10A and MDA-MB-231 cells) were also higher significantly compared to that in normal control cells (without transfection, Figure 11, p<0.05). Moreover, the luciferase activities in co-transfected group were also higher significantly compared to that in single transfected group (Figure 11, p<0.05).

Discussion

Breast cancer is a major health problem as it constitutes the first leading cause for the cancer-associated deaths of females.[1,35] Similar to the other cancers, the pathological mechanism for the breast cancer progression is also elusive and unclear. The previous study reported that the HMGB3 participated in carcinogenesis and progression, such as colorectal cancer, leukemia and gastric cancer.[23,27,36] However, there is little knowledge for the functions of HMGB3 in the progression of breast cancer. Meanwhile, Li et al[37] also found that the downregulation of HMGB3 expression obviously inhibited the urinary bladder cancer cell proliferation and

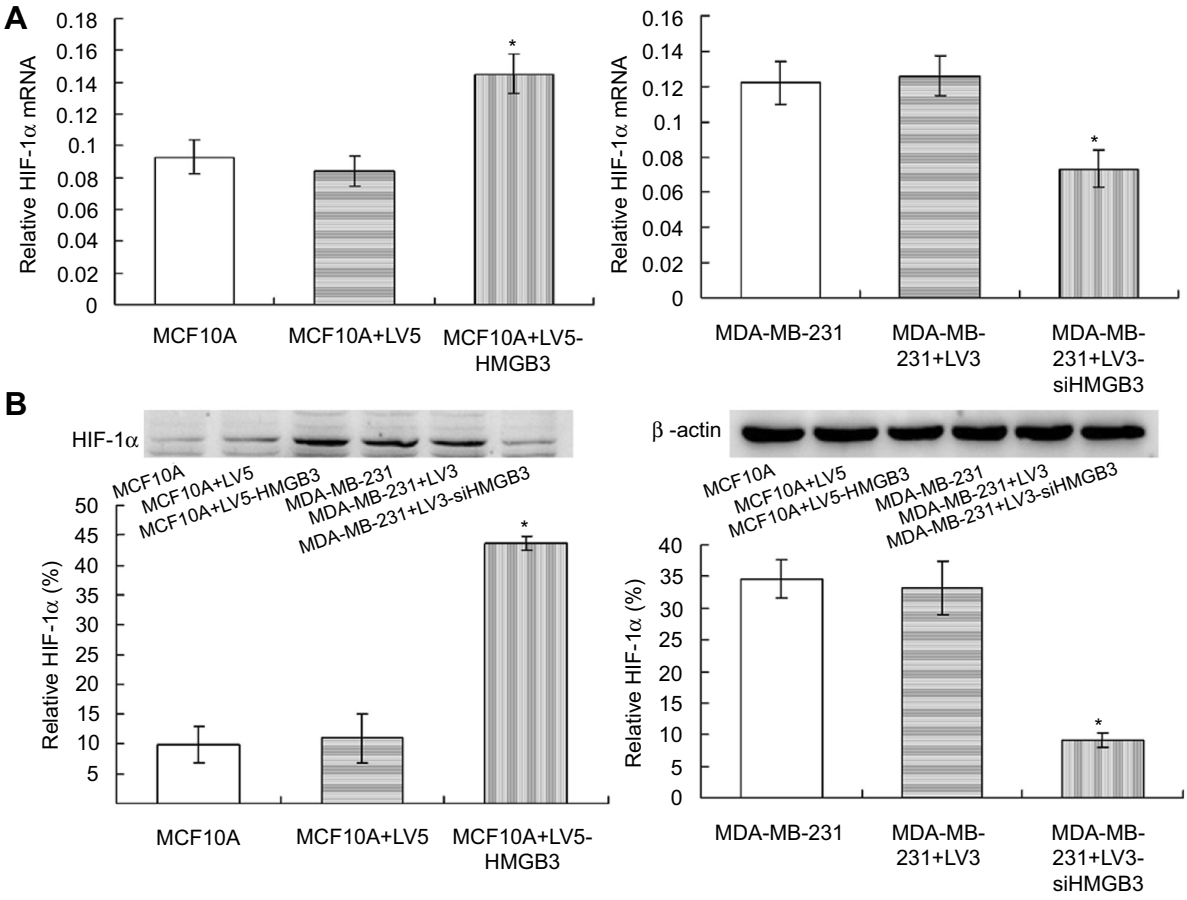

Figure 8 HIF1α examination in the HMGB3-treated MCF10A cells and siHMGB3-treated MDA-MB-231 cells. (**A**). Statistical analysis for HMGB3 mRNA expression. (**B**). Statistical analysis for the HMGB3 expression. *$p<0.05$ *vs* MCF10A cells or MDA-MB-231 cells.
Abbreviation: HMGB3, High-mobility group box 3.

migration. In the present study, we examined the HMGB3 expression and functions in breast cancer cells and clarified the specific mechanism both in vivo and in vitro levels.

In our study, we found that HMGB3 highly expressed in breast cancer cell lines compared to the normal breast cells. Moreover, the HMGB3 expression was also higher significantly in basal-like cell lines (MDA-MB-231, HCC1937) compared to that in luminal cell lines (ZR-75-1, MCF7). Therefore, in the following experiments, we employed the basal-like cell line, MDA-MB-231, to evaluate the functions of HMGB3. The CCK-8 assay showed that HMGB3 overexpression obviously enhanced cell proliferation of MCF10A cells, and HMGB3 silence obviously reduced cell proliferation of MDA-MB-231 cells. These findings suggest that the HMGB3 expression triggers the cell proliferation and HMGB3 inhibition suppresses tumor cell proliferation, which is consistent with a previous study.[38] Meanwhile, the HMGB3 overexpression in MCF10A normal breast cells significantly increased the amounts of mammospheres, and HMGB3 silence in MDA-MB-231 breast cancer cells significantly decreased the amounts of mammospheres. These results suggest that HMGB3 could regulate the mammosphere formation, which is closely associated with tumor migration and proliferation.[39]

A previous study[40] reported that the iPSCs could induce tumor formation. The biomarkers of iPSCs, including Nanog, SOX2 and OCT-4, also participate in tumorigenesis[34] and highly express in highly malignant breast cancer cells.[41] In this study, we found that HMGB3 overexpression significantly increased and HMGB3 silence obviously decreased Nanog, SOX2 and OCT-4 levels, which hint that HMGB3 might be associated with tumor cell proliferation by regulating iPSC biomarker expression. Moreover, former studies[12,13,42] also showed that higher $CD44^+CD24^-$ levels could reflect the tumor cell metastases and mammoshpere formation; therefore, the $CD44^+CD24^-$ levels were examined using flow cytometry. In our study, HMGB3 overexpression enhanced and HMGB3 silence reduced the $CD44^+CD24^-$ levels, which suggests that HMGB3 modulates the $CD44^+CD24^-$ expression in breast cancer cells.

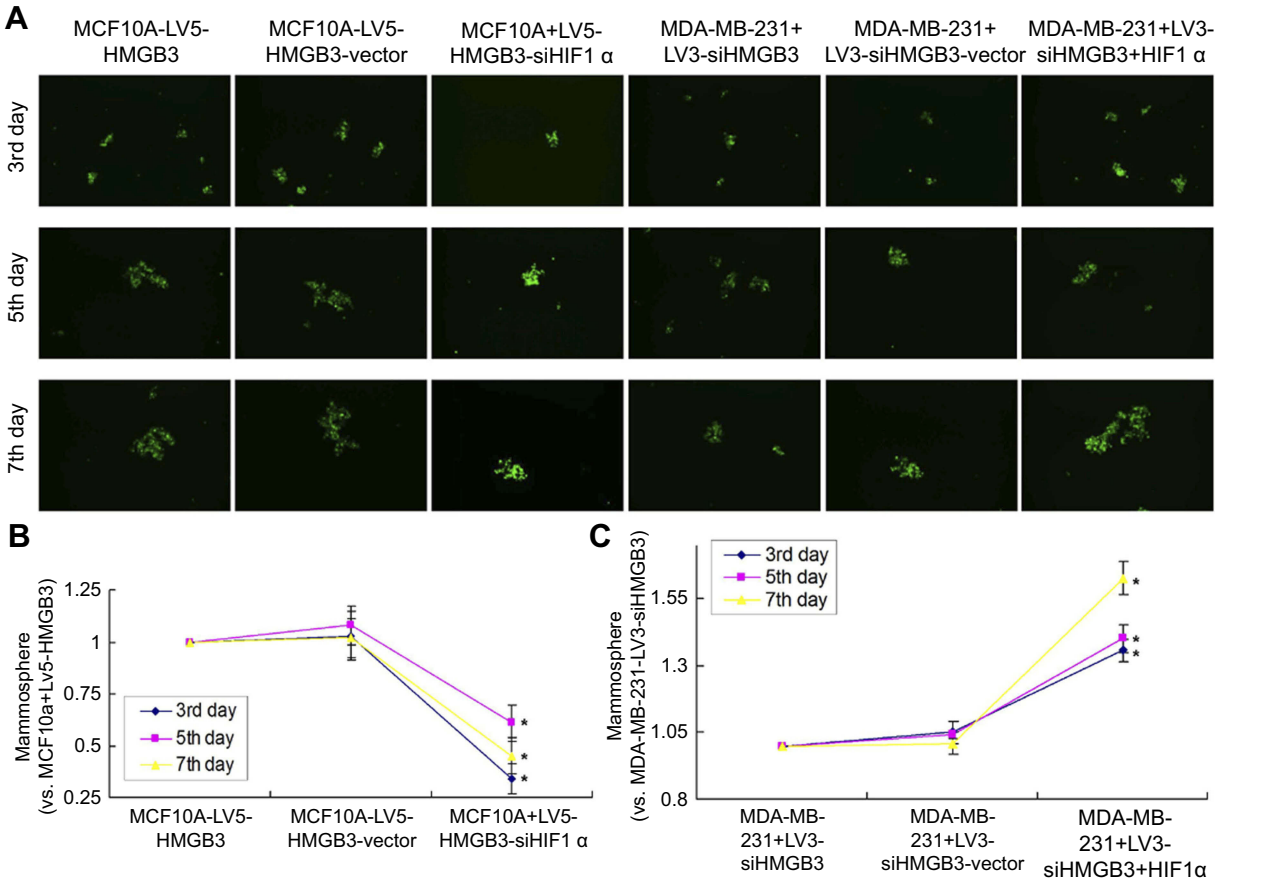

Figure 9 Mammosphere formation in HMGB3/siHIF1α-treated MCF10A cells and siHMGB3/HIF1α-treated MDA-MB-231 cells. (A). Images for the mammosphere formation. (**B**). Statistical analysis for mammosphere formation in HMGB3/siHIF1α-treated MCF10A cells. (**C**). Statistical analysis for mammosphere formation in siHMGB3/HIF1α-treated MDA-MB-231 cells. *p<0.05 vs MCF10A cells or MDA-MB-231 cells.
Abbreviation: HMGB3, High-mobility group box 3.

In the present study, due to the highest HMGB3 expression in the breast cancer cell line, MDA-MB-231 cells, we established the xenograft tumor mouse models by injecting MDA-MB-231 cells. The xenograft tumor mouse models also demonstrated the results that silence of HMGB3 strengthened the reductive effects of PTX on tumor sizes and enhanced the downregulatory effects of PTX on iPSC biomarkers and mammosphere amounts. Therefore, the in vivo experiments suggest that HMGB silence obviously inhibited the growth of the MDA-MB-231 cell-initiated tumors. Actually, the PTX has been proven to be an effective drug for suppressing the tumor cell proliferation according to the previous study.[43] Therefore, in the following study, the investigations for exploring antitumor effects would be further conducted, even in clinical trials.

The above in vivo and in vitro assays demonstrated the effects of HMGB3 silence on tumor growth (proliferation) and levels of tumor-associated biomarkers; however, the actual mechanism was not clarified. Actually, HMGB3 may not regulate the above biomarker directly. The previous study reported that HIF-1α mediated the increased Nanog, Sox2 and OCT-4 expression in the tumor cells in response to the hypoxia.[44] Thus, in the following experiments, we evaluated the effects of HMGB3 silence on the HIF-1α and regulatory effects of siHIF-1α on breast cancer cell proliferation.

Our results indicated that HMGB3 overexpression in MCF10A cells significantly upregulated HIF-1α expression, and HMGB3 silence in MDA-MB-231 cells significantly downregulated HIF-1α expression. Moreover, the findings also showed that the siHIF-1α remarkably eliminated the HMGB3 overexpression causing enhanced amounts of mammoshperes and increased levels of $CD44^{+}CD24^{-}$ in the normal breast cell, MCF10A. Also, the siHIF-1α overexpression significantly enhanced the HMGB3 silence induced decreased amounts of mammoshperes and increased levels of $CD44^{+}CD24^{-}$ in the breast cancer cell, MDA-MB-231 cells. These findings suggest that siHIF-1α plays critical roles in the tumor growth or

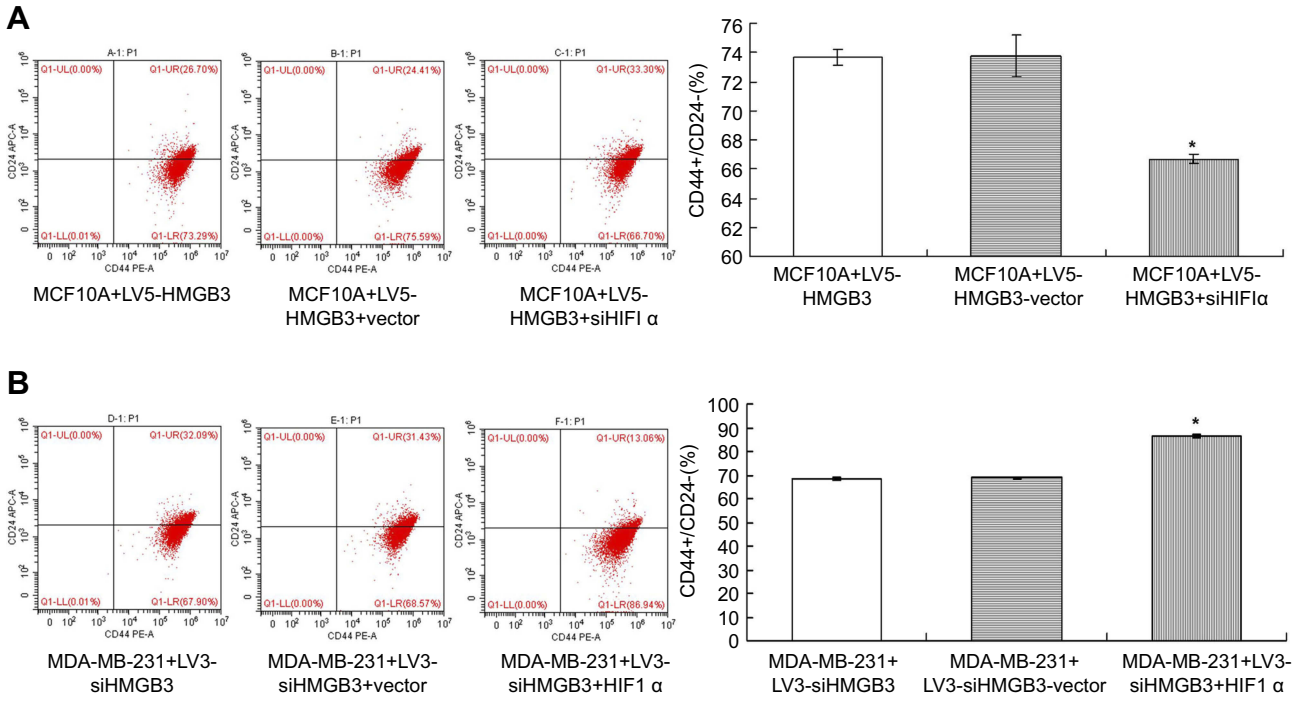

Figure 10 Determination for $CD44^+/CD24^-$ levels in HMGB3/siHIF1α-treated MCF10A cells and siHMGB3/HIF1α-treated MDA-MB-231 cells using flow cytometry assay. (**A**). $CD44^+/CD24^-$ evaluation in HMGB3/siHIF1α-treated MCF10A cells. (**B**). $CD44^+/CD24^-$ evaluation in siHMGB3/HIF1α-treated MDA-MB-231 cells. *p<0.05 vs MCF10A cells or MDA-MB-231 cells.
Abbreviation: HMGB3, High-mobility group box 3.

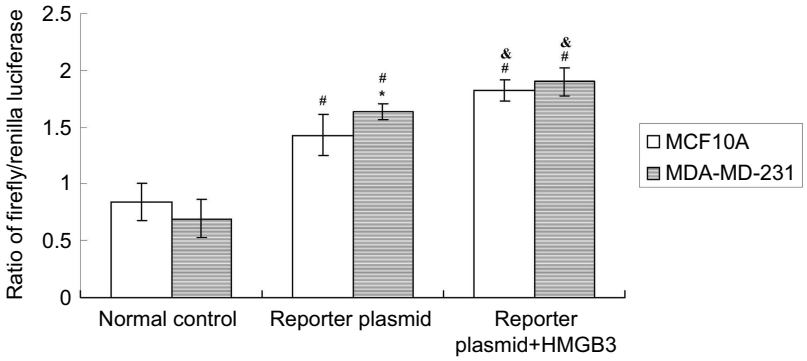

Figure 11 Interaction analysis between HIF1α and HMGB3 expression in MCF10A and MDA-MB-231 cells. *p<0.05 *vs* MCF10A cells. #p<0.05 *vs* Normal control group for both MCF10A and MDA-MD-231 cells. &p<0.05 *vs* single transfected MCF10A or MDA-MB-231 cells.
Abbreviation: HMGB3, High-mobility group box 3.

tumor cell proliferation and overexpression of siHIF-1α could obviously enhance tumor cell proliferation, which are consistent with the previous studies.[45,46] Our results also proved that the HMGB3 interacted with HIF1α in MDA-MB-231 cells, which could explain the effects of HMGB3 on the tumor cell proliferation and mammosphere formation.

Although this study received some interesting results, there were also a few limitations. First, the present study demonstrated the antitumor effects of HMGB3 silence on tumor growth via inhibiting HIF1α, but without mechanism investigation. In the following study, we would investigate the mechanism of HMGB3 silence (or HMGB3 overexpression)-triggered anti-tumor effects, by exploring the signaling pathways, such as AKT/PI3K, MAPK, EMT or JAK2/Stat3 signaling pathways. Second, this study only investigated the effects of HMGB3 silence on cancer cell proliferation and mammosphere formation, but not on cancer cell apoptosis. We would evaluate the apoptosis of cancer cells using caspase 3 analysis and TUNEL analysis. Third, the length of β-actin was relatively long (200 bp) for qRT-PCR assay, which might affect the quantity of results. In a future study, we would

conduct western blotting assay to confirm qRT-PCR results. Fourth, this study has not explained the comparison between basal-like cell lines (MDA-MB-231 and HCC1937) and luminal cell lines (ZR-75-1 and MCF7). Fifth, we only detected the gene and protein expression of HIF1α in the xenografts. In the following study, we would also examine the other associated markers in xenografts. Sixth, this study has not compared the antitumor effects between siHMGB3 treatment and PTX treatment directly, but only clarified the synergistic effects of siHMGB3 on PTX for antitumor effects.

Conclusion

In conclusion, HMGB3 is a critical regulator for tumor growth in breast cancer cells. We found that HMGB3 silence inhibited the mammoshpere formation, cell proliferation and $CD44^{+}CD24^{-}$ levels in breast cancer cells in both in vivo and in vitro levels. The HMGB3 silence played the inhibitive effects on tumor cells by interacting with HIF1α expression in tumor cells.

Disclosure

The authors report no conflicts of interest in this work.

References

1. Vikas P, Borcherding N, Zhang W. The clinical promise of immunotherapy in triple-negative breast cancer. *Cancer Manag Res*. 2018;10:6823–6833. doi:10.2147/CMAR.S185176
2. Vazquez Rodriguez G, Abrahamsson A, Jensen LD, Dabrosin C. Estradiol promotes breast cancer cell migration via recruitment and activation of neutrophils. *Cancer Immunol Res*. 2017;5(3):234–247. doi:10.1158/2326-6066.CIR-16-0150
3. Jemal A, Bray F, Center MM, Ferlay J, Ward E, Forman D. Global cancer statistics. *CA Cancer J Clin*. 2011;61(1):69–90. doi:10.3322/caac.20107
4. Huang ZZ, Chen WQ, Wu CX, et al. Incidence and mortality of female breast cancer in China, a report from 32 Chinese cancer registries, 2003-2007. *Tumor*. 2012;32:435–439.
5. Mayer IA, Abramson VG, Lehmann BD, Pietenpol JA. New strategies for triple-negative breast cancer-deciphering the heterogeneity. *Clin Cancer Res*. 2014;20(4):782–790. doi:10.1158/1078-0432.CCR-13-0583
6. Shan NL, Wahler J, Lee HJ, et al. Vitamin D compounds inhibit cancer stem-like cells and induce differentiation with triple negative breast cancer. *J Steroid Biochem Mol Biol*. 2017;173(1):122–129. doi:10.1016/j.jsbmb.2016.12.001
7. Bianchini G, Balko JM, Mayer IA, Sanders ME, Gianni L. Triple-negative breast cancer, challenges and opportunities of a heterogeneous disease. *Nat Rev Clin Oncol*. 2016;13(11):674–690. doi:10.1038/nrclinonc.2016.66
8. Pogoda K, Niwinska A, Murawska M, Pienkowski T. Analysis of pattern, time and risk factors influencing recurrence in triple-negative breast cancer patients. *Med Oncol*. 2013;30(1):388. doi:10.1007/s12032-012-0388-4
9. Pal S, Luchtenborg M, Davies EA, Jack RH. The treatment and survival of patients with triple negative breast cancer in London population. *Springerplus*. 2014;3(1):553. doi:10.1186/2193-1801-3-553
10. Ji P, Zhang Y, Wang SJ, et al. CD44hiCD24lo mammosphere-forming cells from primary breast cancer display resistance to multiple chemotherapeutic drugs. *Oncol Rep*. 2016;35(6):3293–3302. doi:10.1186/bcr2106
11. Laranjo M, Carvalho MJ, Costa T, et al. Mammospheres of hormonal receptor positive breast cancer diverge to triple-negative phenotype. *Breast*. 2018;38(1):22–29. doi:10.1016/j.breast.2017.11.009
12. Dontu G, Abdallah WM, Foley JM, et al. In vitro propagation and transcriptional profiling of human mammary stem/progenitor cells. *Genes Dev*. 2003;17(10):1253–1270. doi:10.1101/gad.1061803
13. Wahler J, So JY, Cheng LC, Maehr H, Uskokovic M, Suh N. Vitamin D compounds reduce mammoshpere formation and decrease expression of putative stem cell markers in breast cancer. *J Steroid Biochem Mol Biol*. 2015;148(1):148–155. doi:10.1016/j.jsbmb.2014.10.016
14. Ma F, Li H, Shi X, et al. Enriched CD44(+)/CD24(-) population drives the aggressive phenotypes presented in triple-negative breast cancer (TNBC). *Cancer Lett*. 2014;353(2):153–159. doi:10.1016/j.canlet.2014.06.022
15. Rappa G, Lorico A. Phenotypic characterization of mammosphere forming cells from the human MA-11 breast cancinoma cell line. *Exp Cell Res*. 2010;316(9):1576–1586. doi:10.1016/j.yexcr.2010.01.012
16. Grimshaw MJ, Cooper L, Papazisis K, et al. Mammosphere culture of metastatic breast cancer cells enriches for tumorigenic breast cancer cells. *Breast Cancer Res*. 2008;10(3):R52. doi:10.1186/bcr2106
17. Ma R, Karthik GM, Lovrot J, et al. Estrogen receptor beta as a therapeutic target in breast cancer stem cells. *J Natl Cancer Inst*. 2017;109(3):1–14. doi:10.1093/jnci/djw236
18. Gilkes DM, Semenza GL. Role of hypoxia-inducible factors in breast cancer metastasis. *Future Oncol*. 2013;9(11):1623–1636. doi:10.2217/fon.13.92
19. Wang W, He YF, Sun QK, et al. Hypoxia-inducible factor 1α in breast cancer prognosis. *Clin Chim Acta*. 2014;428(1):32–37. doi:10.1016/j.cca.2013.10.018
20. Nemeth MJ, Gurtis DJ, Kirby MR, et al. Hmgb3: an HMG-box family member expressed in primitive hematopoietic cells that inhibits myeloid and B-cell differentiation. *Blood*. 2003;102(4):1298–1306. doi:10.1182/blood-2002-11-3541
21. Costa-Sliva B, Aiello NM, Ocean AJ, et al. Pancreatic cancer exosomes initiate pre-metastatic niche formation in the liver. *Nat Cell Biol*. 2015;17(6):816–826. doi:10.1038/ncb3169
22. Gao J, Zou Z, Gao J, et al. Increased expression of HMGB3: a novel independent prognostic marker of worse outcome in patients with esophageal squamous cell carcinoma. *Int J Clin Exp Pathol*. 2015;8(1):345–352.
23. Gong Y, Cao Y, Song L, Zhou J, Wang C, Wu B. HMGB3 characterization in gastric cancer. *Genet Mol Res*. 2013;12(4):6032–6039. doi:10.4238/2013.December.2.1
24. Staal FJ, de Ridder D, Szczepanski T, et al. Genome-wide expression analysis of paired diagnosis-relapse samples in ALL indicates in involvement of pathways related to DNA replication, cell cycle and DNA repair, independent of immune phenotype. *Leukemia*. 2010;24(3):491–499. doi:10.1038/leu.2009.286
25. Li X, Wu Y, Liu A, Tang X. MiR-27b is epigenetically downregulated in tamoxifen resistant breast cancer cells due to promoter methylation and regulates tamoxifen sensitivity by targeting HMGB3. *Biochem Biophys Res Commun*. 2016;477(4):768–773. doi:10.1016/j.bbrc.2016.06.133
26. Elgamal OA, Park JK, Gusev Y, et al. Tumor suppressive function of mir-205 in breast cancer is linked to HMGB3 regulation. *PLoS One*. 2013;8(10):e76402. doi:10.1371/journal.pone.0076402
27. Zhang Z, Chang Y, Zhang J, et al. HMGB3 promotes growth and migration in colorectal cancer by regulating WNT/β-catenin pathway. *PLoS One*. 2017;12(7):e0179741. doi:10.1371/journal.pone.0179741
28. Nemeth MJ, Kirby MR, Bodine DM. HMGB3 regulates the balance between hematopoietic stem cell self-renewal and differentiation. *Proc Natl Acad Sci USA*. 2006;103(37):13783–13788. doi:10.1073/pnas.0604006103

29. Wang L, Zhai W, Yang X, et al. Lentivirus-mediated stable Fas gene silencing in human umbilical cord-derived mesenchymal stem cells. *Nan Fang Yi Ke Da Xue Bao*. 2014;34(10):1475–1480.
30. Livak KJ, Schmittgen TD. Analysis of relative gene expression data using real-time quantitative PCR and the $2^{-\triangle\triangle ct}$ method. *Methods*. 2001;25(4):402–408. doi:10.1006/meth.2001.1262
31. Shaw FL, Harrison H, Spence K, et al. A detailed mammosphere assay protocol for the quantification of breast stem cell activity. *J Mammary Gland Biol Neoplasia*. 2012;17(2):11–117. doi:10.1007/s10911-012-9255-3
32. So JY, Lee HJ, Smokarek AK, et al. A novel gemini vitamin D analog represses the expression of a stem cell marker CD44 in breast cancer. *Mol Pharmacol*. 2011;79(3):360–367. doi:10.1124/mol.110.068403
33. Qiu Y, Yu Q, Liu Y, et al. Dual receptor targeting cell penetrating peptide modified liposome for glioma and breast cancer postoperative recurrence therapy. *Pharm Res*. 2018;35(7):130. doi:10.1007/s11095-018-2399-0
34. Prieto-Vila M, Yan T, Calle AS, et al. iPSC-derived cancer stem cells provide a model of tumor vasculature. *Am J Cancer Res*. 2016;6(9):1906–1921.
35. Zhu X, Rao X, Yao W, Zou X. Downregulation of MiR-196b-5p impedes cell proliferation and metastasis in breast cancer through regulating COL1A1. *Am J Transl Res*. 2018;10(10):3122–3132.
36. Petit A, Ragu C, Della-Valle V, et al. NUP98-HMGB2: a novel oncogenic fusion. *Leukimia*. 2010;24(3):654–658. doi:10.1038/leu.2009.241
37. Li M, Cai Y, Zhao H, et al. Overexpression of HMGB3 protein promotes cell proliferation, migration and is associated with poor prognosis in urinary bladder cancer patients. *Tumor Biol*. 2015;36(6):4785–4792. doi:10.1007/s13277-015-3130-y
38. Zheng WJ, Yao M, Fang M, Wang L, Dong ZZ, Yao DF. Abnormal expression of HMGB3 is significantly associated with malignant transformation of hepatocytes. *World J Gastroenterol*. 2018;24(32):3650–3662. doi:10.3748/wjg.v24.i32.3650
39. Yang Z, Zhang Y, Tang T, et al. Transcriptome profiling of panc-1 spheroid cells with pancreatic cancer stem cells properties cultured by a novel 3D semi-solid system. *Cell Physiol Biochem*. 2018;47(5):2109–2125. doi:10.1159/000491479
40. Katsukawa M, Nakajima Y, Fukumoto A, Doi D, Takahashi J. Fail-safe therapy by gamma-ray irradiation against tumor formation by human induced pluripotent stem cell-derived neural progenitors. *Stem Cell Dev*. 2016;25(11):815–825. doi:10.1089/scd.2015.0394
41. Ben-Porath I, Thomson MW, Carey VJ, et al. An embryonic stem cell like gene expression signature in poorly differentiated aggressive human tumors. *Nat Genet*. 2008;40(5):499–507. doi:10.1038/ng.127
42. Abraham BK, Fritz P, McClellan M, Hauptvogel P, Athelogou M, Brauch H. Prevalence of CD44+/CD24-/low cells in breast cancer may not be associated with clinical outcome but may favor distant metastasis. *Clin Cancer Res*. 2005;11(3):1154–1159.
43. Ho CM, Lee FK, Huang SH, Cheng WF. Everolimus following 5-aza-2-deoxycytidine is a promising therapy in paclitaxel-resistant clear cell carcinoma of the ovary. *Am J Cancer Res*. 2018;8(1):56–69.
44. Zhang C, Samanta D, Lu H, et al. Hypoxia induces the breast cancer stem cell phenotype by HIF-dependent and ALKBH5-mediated mA-demethylation of NANONG mRNA. *Proc Natl Acad Sci USA*. 2016;113(14):E2047–E2056. doi:10.1073/pnas.1602883113
45. Cai X, Ding H, Liu Y, et al. Expression of HMGB2 indicates worse survival of patients and is required for the maintenance of warburg effect in pancreatic cancer. *Acta Biochem Biophys Sin (Shanghai)*. 2017;49(2):119–127.
46. Zhang Y, Yan J, Wang L, et al. HIF-1 alpha promotes breast cancer cell MCF7 proliferation and invasion through regulating miR-210. *Cancer Biother Radiopharm*. 2017;32(8):297–301. doi:10.1089/cbr.2017.2270